4th International Conference on Integrating GIS and Environmental Modeling (GIS/EM4): Problems, Prospects and Research Needs. Banff, Alberta, Canada, September 2 - 8, 2000.

Developing and integrating advanced GIS techniques in an adaptive grid air quality model to reduce uncertainty

GIS/EM4 No. 188

Maudood Naeem Khan
Mehmet Talat Odman
Hassan Karimi
Michael Goodchild

Abstract

An adaptive grid model is being developed to reduce the uncertainty in air quality predictions. By clustering the grid nodes in regions that would potentially have large errors in pollutant concentrations, the model is expected to generate much more accurate results than its fixed, uniform grid counterparts. The repositioning of grid nodes is performed automatically through the use of a weight function that assumes large values when the curvature (change of slope) of the pollutant fields are large. While the nodes move, the structure of the grid does not change: each node retains its connectivity to the same neighboring nodes. Since there is no a priori knowledge of the grid movement, the input data must be re-gridded after each adaptation step, throughout the simulation. Pollutant emissions are one of the major inputs to the model. Mapping the emissions from power plant stacks, highways and other area sources requires the use of GIS. Efficient intersection algorithms are being developed that take advantage of the unchanging structure of the grid.

In this paper, both the grid node repositioning and the intersection algorithms are evaluated in an application to terrain elevation data. The data set for the island of Hawaii, which is originally at 4x4 km resolution, is compressed to one fourth of its size using grid node repositioning. The maximum and cumulative errors due to this compression are respectively 60% and 25% smaller than uniform grid compression with 8x8 km resolution. While this result shows that the algorithms have the potential of significantly improving the accuracy of air quality predictions, computational efficiency implies that the overhead should not be limiting in air quality simulations.

Keywords

Air quality model, adaptive grids, intersection algorithms, emissions, nested grids

Introduction

Air quality models (AQMs) play a central role in the design of emission control strategies that are being developed to improve air quality. It is important to improve the accuracy of AQM predictions not only because the control strategies are costly to implement but also because they have a direct bearing on public health and lifestyle. A great deal of the uncertainty in predictions is attributed to the resolution of the numerical grid, which is limited by the availability of computational resources. A large grid size is unable to resolve input data or capture the non-linear physical and chemical processes that occur over smaller spatial scales. To address this issue, nested grid or multi-scale modeling techniques have been developed that use finer grid resolution in regions of interest and coarser grids elsewhere (Odman et al. 1997). These techniques are limited by not

knowing, a priory, where to place the finer resolution grids, loss in solution accuracy due to grid interface problems (Alapaty et al. 1998), and the inability to adjust to dynamic changes in the solution. An alternative approach to achieving local resolution involves using dynamic adaptive grids, which are not subject to the aforementioned limitations. Using a weight function that represents the error in the solution, grid nodes are clustered in regions where they are needed the most. Once the grid nodes are repositioned, the numerical solution is computed with greater accuracy compared to a fixed grid.

Probably the most restrictive issue in the development of adaptive grid AQMs is the processing of emissions for a continuously moving grid. Emission inventories include hundreds of compounds emitted from a variety of sources ranging from large utility plants to motor vehicle tailpipes. Geographical Information Systems (GIS) are used to retrieve the raw emissions data from the inventories and generate gridded, time-varying emissions in terms of the chemical species represented in the models. In adaptive grid models, the shape and location of grid cells change after each adaptation. A source that lies in a grid cell might lie in another cell after adaptation. Therefore, the processing of emissions data must be performed in real time, after each adaptation of the grid. The task of locating a point (e.g., stacks), line (e.g., roads) or an area (e.g., farm) source within a grid is referred to as the intersection problem. Efficient intersection algorithms are needed to compensate for the real-time overhead of re-gridding emission inputs.

This paper describes the grid repositioning and intersection algorithms, and discusses their performance in a test problem consisting of adapting a grid to terrain elevation data. The major difference between an elevation field and a pollutant field is that the former is static while the latter changes in time. In AQM simulations, the evolution of pollutant fields is captured in discrete time steps. Each time step is followed by a grid adaptation step such that the pollutant field can be better resolved. The test emulates a single adaptation step of an actual AQM simulation where time evolution is stopped and the grid is adapted to the pollutant field. Despite this simplification, the similarities between complex terrain and pollutant fields, in terms of changing slopes, makes this test a good evaluation case for the grid-repositioning algorithm. The test case also emulates the intersection of point sources with grid cells in an indirect way. While the elevation of repositioned nodes are calculated, there is a need to intersect each node with the cells of the grid containing the original terrain data.

Methodology

The adaptive grid methodology used here is based on the Dynamic Solution Adaptive Grid Algorithm (Benson and McRae, 1991). It employs a constant number of grid nodes that partition a rectangular domain into N by M quadrilateral grid cells. The nodes move throughout the simulation but the grid structure remains the same. In other words, each node is still connected to the same neighboring nodes but the length of the links and the area of the grid cells change. There is a significant advantage of this method over other adaptive techniques that enrich the mesh by adding grid nodes or use unstructured grids. Since the number of nodes and the grid structure remains the same, the adaptive grid that is non-uniform in the physical space (x,y) can be mapped onto a uniform grid in the computational space (ξ,η) with a transformation of the form

(Notation 1)
$$\xi = \xi(x,y)$$
$$\eta = \eta(x,y)$$

The movement of the nodes is controlled by a weight function whose value is proportional to the error in the solution. The nodes are clustered around regions where the weight function bears large values, thereby increasing the resolution where the error is large. Since the number of nodes is fixed, refinement of grid scales in regions of interest is accompanied by coarsening in other regions where the weight function has smaller values. This yields a continuous multiscale grid where the scales change gradually. Unlike nested grids, there are no grid interfaces, which may introduce numerous difficulties due to the discontinuity of grid scales. The availability of computational resources determines the number of grid nodes that can be afforded in any AQM. By clustering grid nodes automatically in regions of interest, computational resources are used in an optimal fashion throughout the simulation.

Weight Function and Grid Node Repositioning

The grid nodes are moved in the space (ξ,η) using a weight function along with a center-of-mass repositioning scheme. The weight function w(x,y,t) must be such that its value is large in regions where grid nodes need to be clustered. There are also some requirements for the resulting grid in order to assure an accurate numerical solution of governing partial differential equations. The grid must be free of highly skewed cells, and there must be a smooth transition from small to large cells with no voids in regions where the pollutant field is relatively uniform. Laflin and McRae (1996) developed a weight function that satisfies these requirements and is very easy to compute:

(Notation 2) $$w_{i,j} = \nabla^2(\phi)_{i,j} + w_{min}$$

where ∇^2 is a discrete approximation to the Laplacian of the form

(Notation 3) $$\nabla^2(\phi)_{i,j} = \frac{1}{4}\left(\phi_{i-1,j} + \phi_{i+1,j} + \phi_{i,j-1} + \phi_{i,j+1} - 4\phi_{i,j}\right)$$

which also represents the error between the grid node value of field variable ϕ and the value obtained from the interpolation of ϕ values in the neighboring cells. A relatively small value of $\nabla^2\phi$ for any cell indicates that the grid can support relatively accurate interpolations of ϕ in the neighborhood of that cell. A minimum weight, w_{min}, inhibits evacuation of grid nodes from regions of uniform concentration.

The weight function above can result in the formation of concave or highly skewed grid cells. Since such grid cells are undesirable, a diffusive filter is applied to smooth this weight function. The final weight function is obtained by applying an area weighting to the smoothed weight function.

(Notation 4) $$\tilde{w}_{i,j} = A_{i,j}^{1+e}\left(w_{i,j}^{\text{filtered}}\right)$$

The parameter *e* controls weighting with respect to the cell area A: a positive value gives more weight to larger cells and promotes gradual transitions from larger to smaller cells.

Repositioning of the grid nodes is accomplished by a *center-of-mass* scheme, originally proposed by Eiseman (1987). In this scheme, the weight function is viewed as a mass distribution. Consider a new cell definition whose vertices are the original grid cell centers and centroid is the grid node itself. The new position of the grid node, $\vec{P}^{new}$, is defined as the center-of-mass of this newly defined cell:

(Notation 5) $$\vec{P}^{new} = \frac{\sum_{i=1}^{4} w_i \vec{P}_i}{\sum_{i=1}^{4} w_i}$$

where $\vec{P}_i$ are the position vectors of the original cell centers and w_i are the values of the weight function at those locations. The center of mass scheme is computationally very efficient. One disadvantage is that it is possible to have grid line cross-over, if the center of mass is located outside the original cell. However, by repositioning the nodes in the (ξ,η) space, where the grid is uniform, this possibility is eliminated. After all grid nodes are repositioned, the adapted grid is mapped back to the (x,y) space by using the inverse of the transformation in Notation 1.

Finally, if the maximum movement of all grid-nodes is below a preset tolerance, the grid is considered to have resolved the field sufficiently. Otherwise, the weight function is recomputed and the grid adaptation procedure is reiterated. The movement tolerance used here is, for any node, 5% of the distance to the closest node. Note that repositioning the nodes leads to a non-uniform grid in the (ξ,η) space. Reestablishing a uniform computational grid requires a different transformation.

Point Source-Grid Cell Intersection Algorithm

Since the locations of the grid nodes have changed in the physical (x,y) space, input data such as emissions must be re-gridded. As mentioned before, there are three major types of emissions being input into an AQM: emissions from point, line and area sources. Gridding of these emissions requires GISs to find the intersections of each source type with the adapting grid cell. The structure of the grid at hand and the quadrilateral shape of the cells can be exploited to develop efficient intersection algorithms. This way the overhead involved in the re-gridding operations can be significantly reduced.

Intersecting point sources with the grid is the easiest one. A search is conducted over all grid cells to find out which one encloses the point source. The following algorithm has been developed. As illustrated in Figure 1, starting from any vertex, two vectors are drawn: one to the next vertex in the counterclockwise direction and another to the point source location. If the cross product of the first vector with the second vector is negative (in a right-handed coordinate system), then the point source is outside this cell. In this case, checking the sign of the cross product is continued from the neighboring cell that shares with the original cell the side marked by the first vector above. In a structured grid where the cells are stored in an N by M array, finding this element is trivial. If the cross product is positive, the process is continued from the next vertex of the cell. If the process yields positive cross products for all four vertices, then the point is inside that cell.

In general, the adaptive grid is initialized as a uniform grid. During the air quality simulation, the changes in pollutant fields are usually not dramatic enough to require a sudden adaptation from a uniform grid to a grid that can support a very complex field. In other words, the grid node movements would never be as large as they were in the initial adaptation step. In fact, it is very likely that the cell containing the point source prior to grid node repositioning would not move too far away from that source. Therefore, the point source can be located much faster by starting the search from the cell where it was found in the previous search. Efficient algorithms that take advantage of the topology of

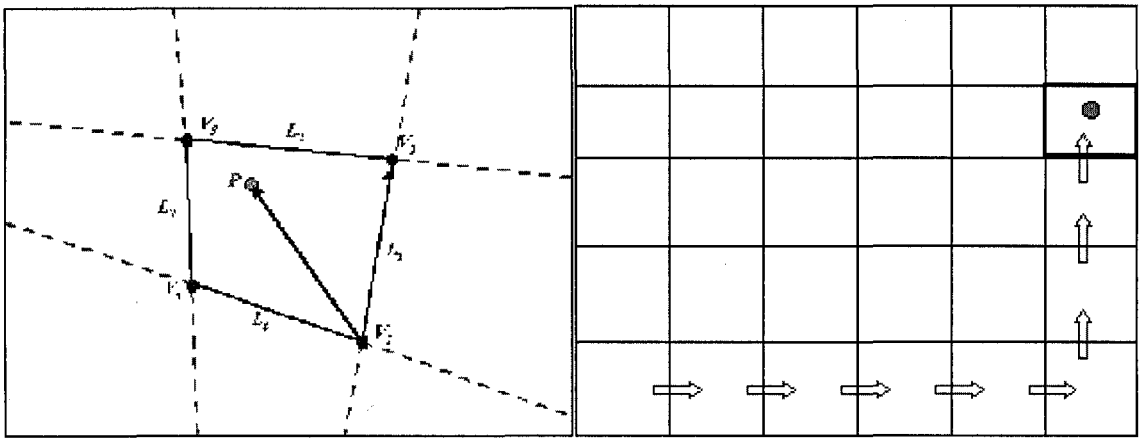

Figure 1. Locating a point P in a grid cell (left). Arrows (blue) indicating the search as it proceeds to locate point *P* in *NxM* grid cells (right).

the grid, as well as the small change in pollutant field assumption, have also been developed for line and area sources. However, they are not discussed in this paper.

Application to Surface Elevation Data

The surface elevation over complex terrain resembles pollutant concentration fields in many ways. Over large regions of flat terrain such as oceans, lakes, valleys and plains, there are local features with large curvature in coastal areas, foothills, and mountain peaks. The only notable difference is that surface elevation is constant over time. However, recall that the grid adaptation procedure is applied by freezing the evolution of the pollutant field, thus, at any instant, the complexity of a pollutant field can be well represented by a surface elevation field. The accuracy of surface elevation data for any geographical location depends on the resolution of the grid. A finer resolution grid can follow the changes in slope more closely than a coarser grid. Increasing the resolution uniformly over the entire domain may not be desirable since data storage requirements are proportional to the square of linear resolution. The adaptive grid method above offers a more efficient solution by increasing the resolution only in regions of large curvature.

Application to the Island of Hawaii

The surface elevation data from the Digital Elevation Model (DEM) for a region surrounding the Island of Hawaii was processed onto a uniform 120x120-cell fine grid with a 4-km resolution. The same data was also mapped on a coarse grid with 60x60-grid cells, and uniform 8-km resolution. This second grid serves as the static grid with which the adaptive grid is compared. It also constitutes the starting point for the adaptive grid. A weight function was computed based on the curvature of the terrain and the grid nodes were repositioned. After the coordinates of the adapted grid are computed in the physical space, the elevation of the grid nodes was obtained by bilinear interpolation from the fine grid. During this procedure, it is necessary to find the fine grid cell containing any given node of the adaptive grid. For this, we used the above described intersection algorithm developed to search for the grid cell that contains a given point.

In order to assess if the adapted grid captures the surface elevation more accurately than the coarse grid, which is static and uniform, surface elevation from both grids is interpolated back onto the fine grid. While the interpolation from the coarse grid onto the fine grid is performed only once, the interpolation from the adaptive grid to the fine grid is performed every time the grid nodes are repositioned. Thus, after each iteration, there are three sets of surface elevation data on the fine grid: one from the DEM data set, another that is interpolated from the coarse grid, and a third one interpolated from the adaptive grid. These data sets are used in calculating and comparing the errors from the adaptive and coarse grids. The adaptation process is continued until all the node movements are below the preset relative tolerance.

Discussion of results

The evolution of the grid during the adaptation process was visualized to see the grid-repositioning algorithm created any highly skewed cells or voids in areas of flat terrain. The grid node movements were large in the beginning, but they decreased exponentially as shown in Figure 2. The grid movement tolerance was achieved after 375 iterations.

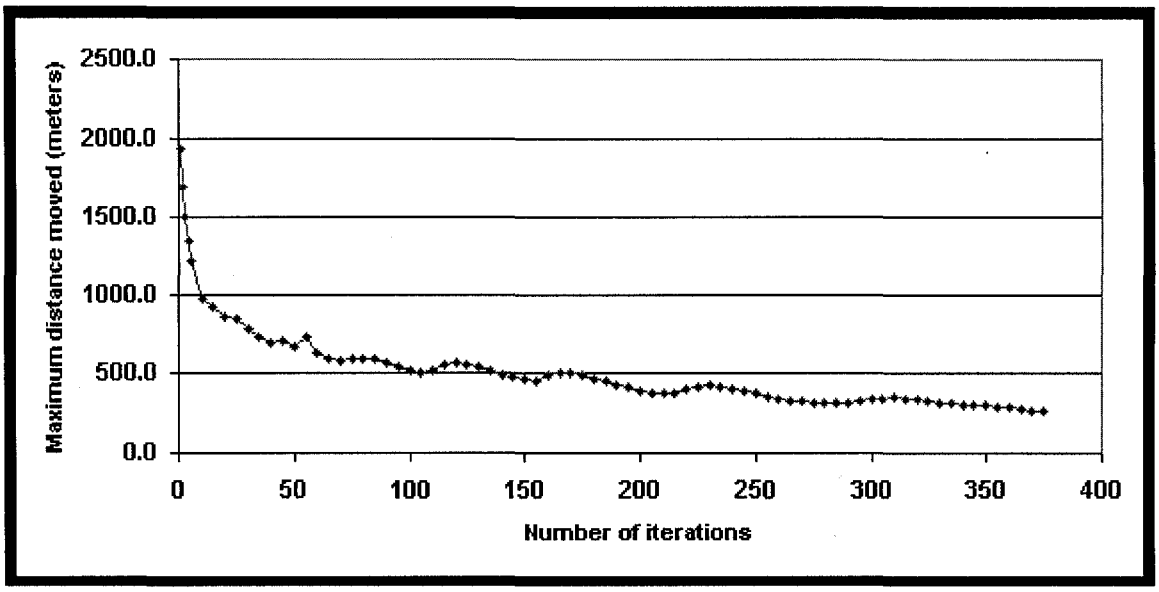

Figure 2. Maximum distance moved by any grid node as a function of grid repositioning iterations.

The surface elevation of the domain and the final configuration of the grid are shown in Figure 3. In general, the grid nodes are clustered in regions with abrupt changes in surface elevation. The transitions from coarse to fine resolution (or vice versa) are smooth and no highly skewed cells or voids are visible.

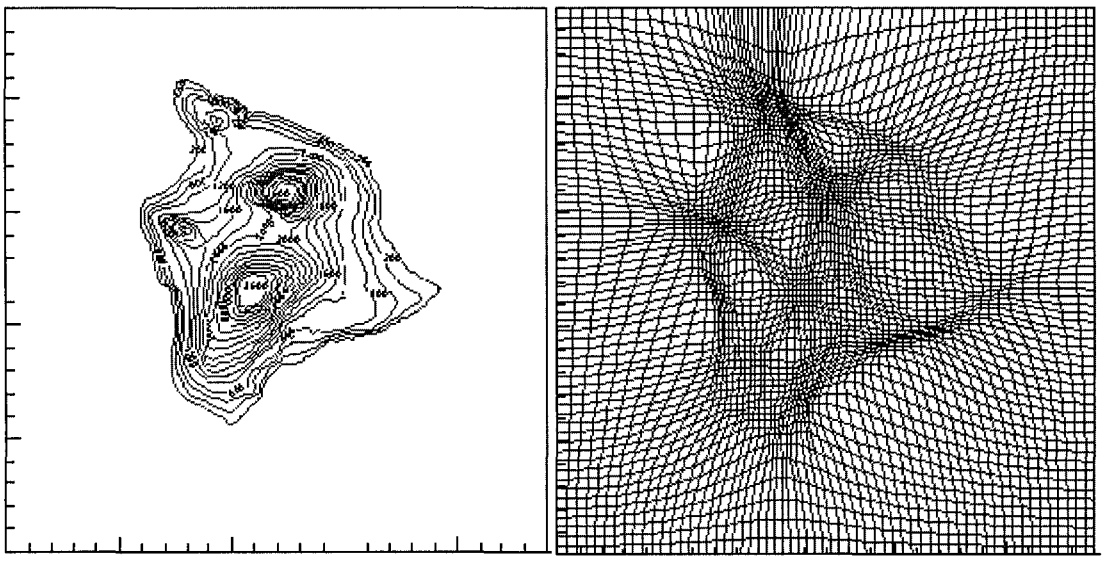

Figure 3. Surface elevation for the island of Hawaii (left) and the grid adapted to the terrain features (right).

The difference between the interpolated surface elevation (either from the adaptive grid or from the coarse grid onto the fine grid) and the value from DEM data at any fine grid node is defined as the nodal error:

(Notation 6) $$E_{i,j} = \left| \phi_{i,j}^{DEM} - \phi_{i,j}^{ADAPTIVE} \right|$$

The maximum nodal error decreases from the initial value of 520 m, which is also the maximum error for the

coarse grid, to 198 m after 375 iterations (Figure 4). The increases in maximum error after periods of monotonic decrease correspond to shifts in maximum error from one area of the geographic domain to another. Recall that, since the number of nodes is fixed, the adaptive grid algorithm is clustering the nodes around one terrain feature at the expense of decreased resolution elsewhere. Therefore, while the local error around one terrain feature is decreased, it may start to increase around some other feature. However, there is a decreasing trend in the global maximum error, which is promising. This trend shows that the grid is converging towards a state where the domain-wide maximum error is minimized, although the final grid, which satisfied the node movement tolerance, does not correspond to the minimum local error. In order to reduce the maximum error below 198 m, which is the minimum in Figure 4, the number of grid nodes would have to be increased.

The cumulative error was also analyzed. After an initial period of increase (up to about the 10th iteration), there is an exponential decrease in cumulative error (Figure 5). The cumulative error was further broken down into its components coming from the nodes that are only present on the fine grid and those that are also on the coarse grid. Clearly, the initial increase in the cumulative error is coming from those latter nodes. Recall that the adaptive grid was initially the same as the coarse grid and that the surface elevation

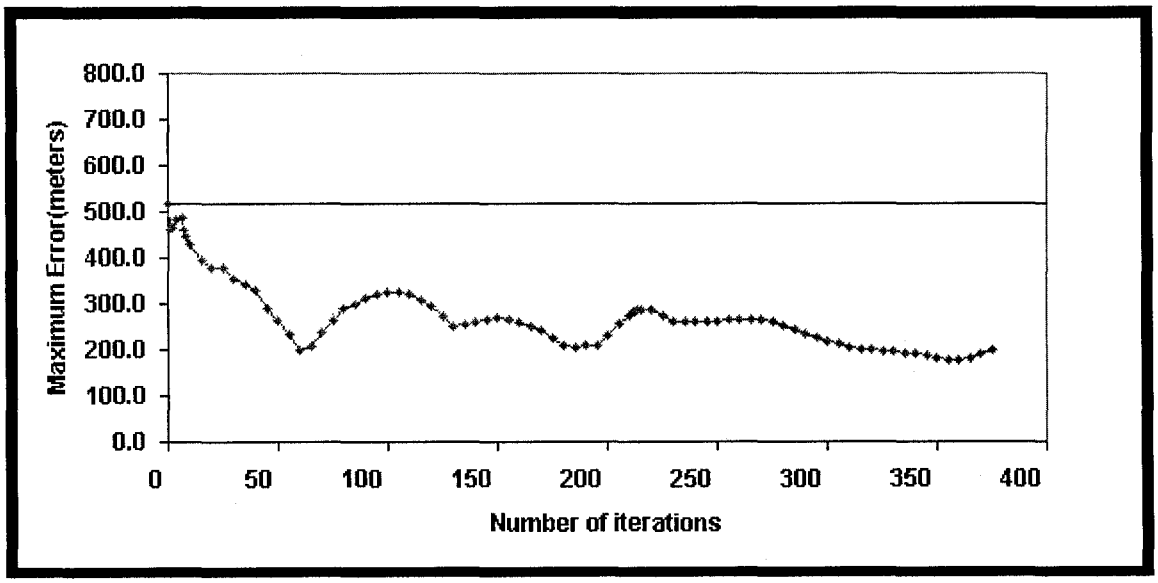

Figure 4. Maximum error as a function of grid repositioning iterations.

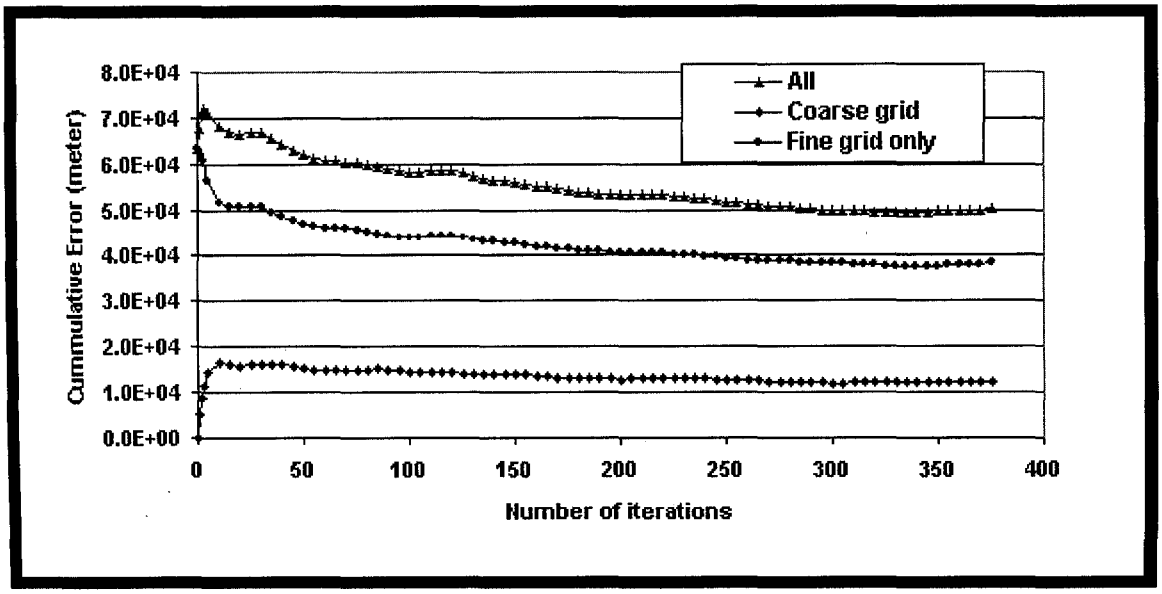

Figure 5. Cumulative error and its breakdown to the nodes that are also on the coarse grid and those that are only present on the fine grid.

values for all the nodes were derived from the DEM data. Thus, the error at the nodes shared by the coarse and fine grids is zero. Once the node movement starts, the error at those nodes can only increase, but it reaches a plateau after about 15 iterations. Meanwhile, the cumulative error component for the nodes that are only on the fine grid decreases exponentially. At about the 10th iteration, this decrease offsets the increase in the other component, so the overall cumulative error starts decreasing. The monotonic decrease of the cumulative error afterwards show that the grid adaptation is effectively increasing the accuracy of surface elevation, globally. Overall, the cumulative error decreased by more than 25% compared to the initial (coarse) grid.

In summary, the error in representing surface elevation data with four times fewer nodes than the original fine grid is smaller on the adaptive grid than the uniform coarse grid. Maximum error may shift from one location to another several times during the iterative grid-node repositioning process, and it is not necessarily minimized at the end, when the movement tolerance is met. However, the cumulative error decreases almost monotonically indicating that the global error is effectively minimized. The rate of convergence is not very fast, but since the grid node repositioning algorithm is inexpensive (all 375 iterations were completed in 600 seconds on a 200 MHz processor) this does not pause a limitation. The resulting grid fulfills all of the requirements set forth for accurate numerical solution of partial differential equations.

Conclusion

An adaptive grid AQM is being developed. In this paper, the grid node repositioning and the point-source-grid-cell intersection algorithms were evaluated, for both efficiency and accuracy, using terrain elevation data. The algorithms were found efficient enough that the overhead of grid adaptations or re-gridding of emissions should not be restrictive in AQM simulations. The adaptive grid improves the accuracy considerably over a uniform grid with the same number of nodes. The maximum and cumulative errors decreased by more than 60% and 25%, respectively, due to grid adaptations in an application to the terrain of the island of Hawaii. Similar improvements can be expected in AQM results where pollutant fields resemble terrain fields in terms of complexity.

References used

Alapaty K, Mathur R, Odman T. 1998. Intercomparison of spatial interpolation schemes for use in nested grid models. Monthly Weather Review (126):243-249.

Benson RA, McRae DS. 1991. A Solution adaptive mesh algorithm for dynamic/static refinement of two and three dimensional grids. In Proceedings, Third International Conference on Numerical Grid Generation in Computational Field Simulations, Barcelona, Spain, June 1991.

Eiseman PR. 1987. Adaptive grid generation. Computational Methods and Application in Mechanical Engineering (64): 321.

Laflin KR, McRae DS. 1996. Three-dimensional viscous flow computations using near-optimal grid redistribution. In Proceedings, First AFOSR Conference on Dynamic Motion CFD, Rutgers University, New Jersey.

Odman MT, Mathur R, Alapaty K, Srivastava RK, McRae DS, Yamartino RJ. 1997. Nested and adaptive grids for multiscale air quality modeling. In: Delic G, Wheeler MF, editors. Next generation environmental models and computational methods. Philadelphia, PA: SIAM. p 59-68.

Authors

Maudood Naeem Khan, Ph.D Candidate
Georgia Institute of Technology, 200 Bobby Dodd Way, Atlanta, GA 30332.
Email:maudood@themis.ce.gatech.edu, Tel: +1-404-894-3089, Fax: +1-403-894-8266

Mehmet Talat Odman, Senior Research Engineer
Georgia Institute of Technology, 200 Bobby Dodd Way, Atlanta, GA 30332.
Email:talat.odman@ce.gatech.edu, Tel: +1-404-894-2783, Fax: +1-403-894-8266

Hassan Karimi, Assistant Professor
University of Pittsburgh, PA 15260.
Email:hkarimi@mail.sis.pitt.edu, Tel: +1-412-624-4449, Fax: +1-412-624-2788

Micheal F. Goodchild, Professor and Chair
National Center for Geographic Information and Analysis, Santa Barbara, CA 93106.
Email:good@ncgia.ucsb.edu, Tel: +1-805-701-6994, Fax: +1-805-893-3146